AFC 4 Hydro

Active Flow Control system FOR improving Hydraulic turbine performances at off-design Operation

AFC SYSTEM VALIDATED ON A MODEL TURBINE

EUROPEAN COMMISSION Grant Agreement No: 814958 11/30/2023

Xavier Escaler, Xavier Sanchez Botello, Rafel Roig, Joel Sundström, Shahab Shiraghaee, Michel Cervantes, Morten Kjeldsen, Khalid Atta

Grant Agreement No: 814958

DELIVERABLE D4.3

AFC system validated on a model turbine

Description:

The Active Flow Control (AFC) system is composed of various subsystems, encompassing the Injection of Pulsating Momentum (IPM), Injection of Continuous Momentum (ICM), Structural Health Monitoring System (SHM), and the controller. The process of developing these subsystems and integrating them has been executed on a turbine model. The obtained and presented results effectively showcase the capabilities of the developed concept.

Document identifier:	AFC4Hydro_Deliverable_D4_3
Due date:	30/11/2023
Delivery date:	28/11/2023
Work package:	4
Lead beneficiary:	LTU
Dissemination level:	Public

This project has received funding from the European Union's Horizon 2020 research and innovation programme under grant agreement No 814958

Table of contents

1 Introduction

The AFC4Hydro initiative focuses on advancing an innovative Active Flow Control (AFC) system designed to enhance the off-design performance of hydraulic turbines. This is achieved by addressing detrimental flow phenomena during both steady and transient operations, including ramping, with the ultimate goal of boosting reliability, flexibility, and minimizing wear and tear. The AFC system comprises various subsystems, namely the Injection of Pulsating Momentum (IPM), Injection of Continuous Momentum (ICM), Structural Health Monitoring System (SHM), and the controller. The subsystems were initially developed individually at small scales at

- Luleå University of Technology, Sweden, for the IPM and Controller (D1.1 and D4.2)
- Flow Design Bureau, Norway, for the ICM (D2.1)
- Universitat Politècnica de Catalunya, Spain, for the SHM (D3.1)

The next steps in the project consisted in upscaling the different subsystems and merging them. The up-scaling and merging of the different subsystems was planned to be performed at the water laboratory of Vattenfall, Sweden. The up-scaling of the different subsystems was performed on a Kaplan turbine model. Each subsystem development was performed with another subsystem:

- IPM with SHM,
- ICM with SHM
- controller with IPM and SHM

Measurements with the SHM, IPM and ICM were also performed.

This document presents a summary of the outcomes of experiments conducted with the different subsystems (IPM, ICM, SHM, Controller) at the water laboratory, Vattenfall, Sweden.

2 SHM

A Structural Health Monitoring (SHM) system has been used to evaluate the model turbine condition and performance during steady and transient operating conditions. By means of several sensors installed off-board and on-board along the turbine shaft line, a continuous observation and analysis over time of the hydraulic turbine dynamic response has been performed to characterize the turbine state and to monitor its changes during operation under deleterious flow phenomena.

In order to design and optimize the SHM system to be used in the model turbine, a preliminary version of the SHM was developed and installed in a bespoke test rig built at the Barcelona Fluids & Energy Lab (IFLUIDS) laboratory of Universitat Politècnica de Catalunya (UPC). The test rig is composed of a rotating submerged structure with a hollow shaft-disk assembly that replicates the typical shaft-runner assembly of a hydraulic turbine. By means of a DC motor, it can rotate at several speeds and the flow around the disk can be observed through the plexiglass tank of water where it is submerged, see Figure *1*.

Along the stationary and rotating structure, traditional instruments such as accelerometers, displacement sensors, strain gauges and pressure transducers were installed together with innovative transducers such as Fiber Bragg Grating (FBG) sensors. Additionally, methodologies to extract the structural modal response of a rotating and submerged structure were developed using piezoelectric patches attached to the structure, which were used to excite different natural frequencies using chirp signals.

Figure 1 - Bespoke test rig installed in UPC for developing the SHM system

2.1 System implemented

The acquisition and processing of the data was implemented using a real-time embedded industrial controller from National Instruments (NI) called CompactRIO (cRIO). This device offers the flexibility to use different Input/output (I/O) modules to connect a wide variety of sensors. Concretely, the modules tested at the laboratory and finally used at the model turbine are presented in Table 1.

Table 1. NI cRIO acquisition modules used for the measuring campaigns at the model turbine.

NI modules	Description
NI 9231	8 input acceleration channels
NI 9231	8 input acceleration channels
NI 9253	5 input displacement current channels
NI 9223	4 input voltage channels for pressure sensors
NI 9202	16 input voltage channels for strain gauges and pressure sensors
NI 9202	16 input voltage channels for strain gauges and pressure sensors
NI 9205	32 input voltage channels for strain gauges and pressure sensors

A total of 200 sensors were installed in the model turbine at different locations as outlined in Figure *2*. From them, the most sensitive ones to detect the Rotating Vortex Rope (RVR) and the flow instabilities at Speed No Load (SNL) and during starts, stops and ramping of power were acquired by the SHM system, mainly measuring vibrations at the bearing pedestals, displacements of the shaft at several positions, pressures of the draft tube cone at different levels and the strains of the rotating shaft and the runner blades. Additionally, the innovative FBG technology was also installed on the draft tube cone to measure the induced strain levels.

The optimized software used for the SHM system in the model turbine has been based on a LabVIEW application that computes in real-time different health indicators to determine the turbine characteristics and that detects the frequency of the RVR. Using the spectra of the time signal computed in real-time, the RVR frequency can be identified and adjusted in real-time to define the power bands for each strain, vibration and pressure. In addition, the raw data is stored in a TDMS file for the later post-processing of the acquired data. The front panel of the SHM front view on the computer screen in shown in Figure *3*.

The measurements were performed at a fixed blade angle of 1.8º and 0.8º along the propeller curve for different guide vane angles from 18º to 34º. Additionally, SNL measurements were performed with and without cavitation together with different transient measurements from Best Efficiency Point (BEP) to SNL. Measurements were taken without any injection system to obtain the reference levels and also with the actuation of the IPM and ICM separately and together in order to quantify their effects.

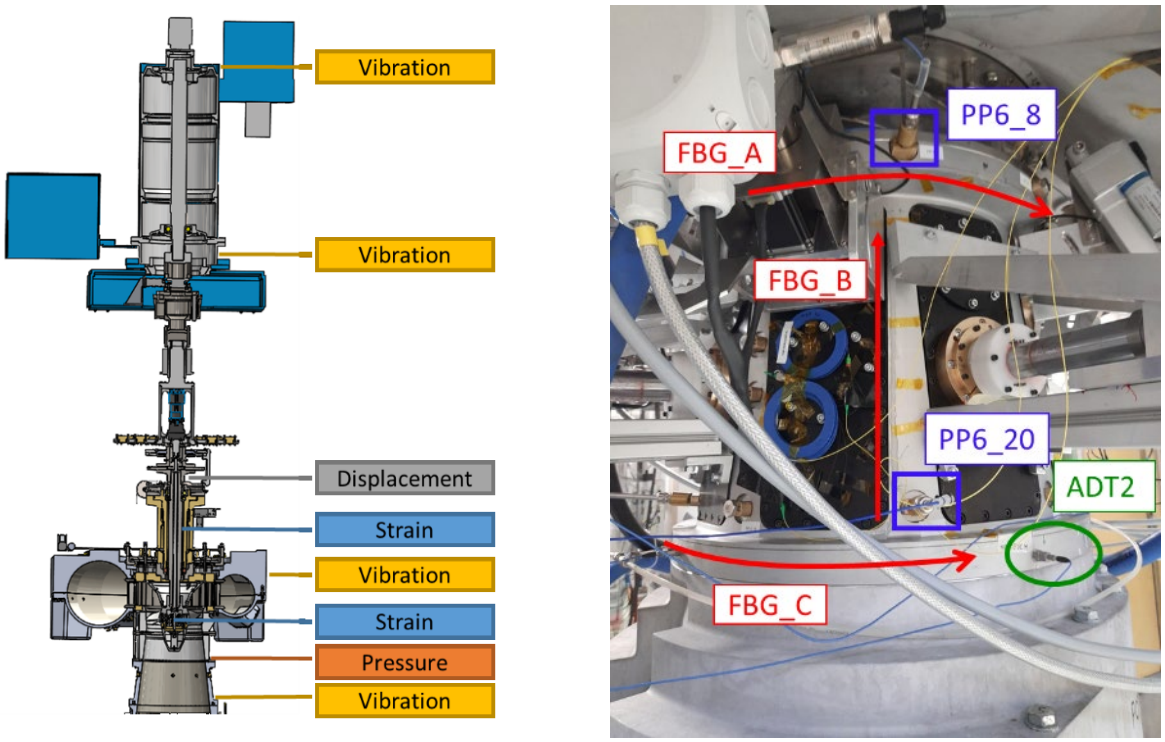

(a) (b)

Figure 2 - Scheme of the type of sensors installed along the model turbine (a) and in the draft tube (b).

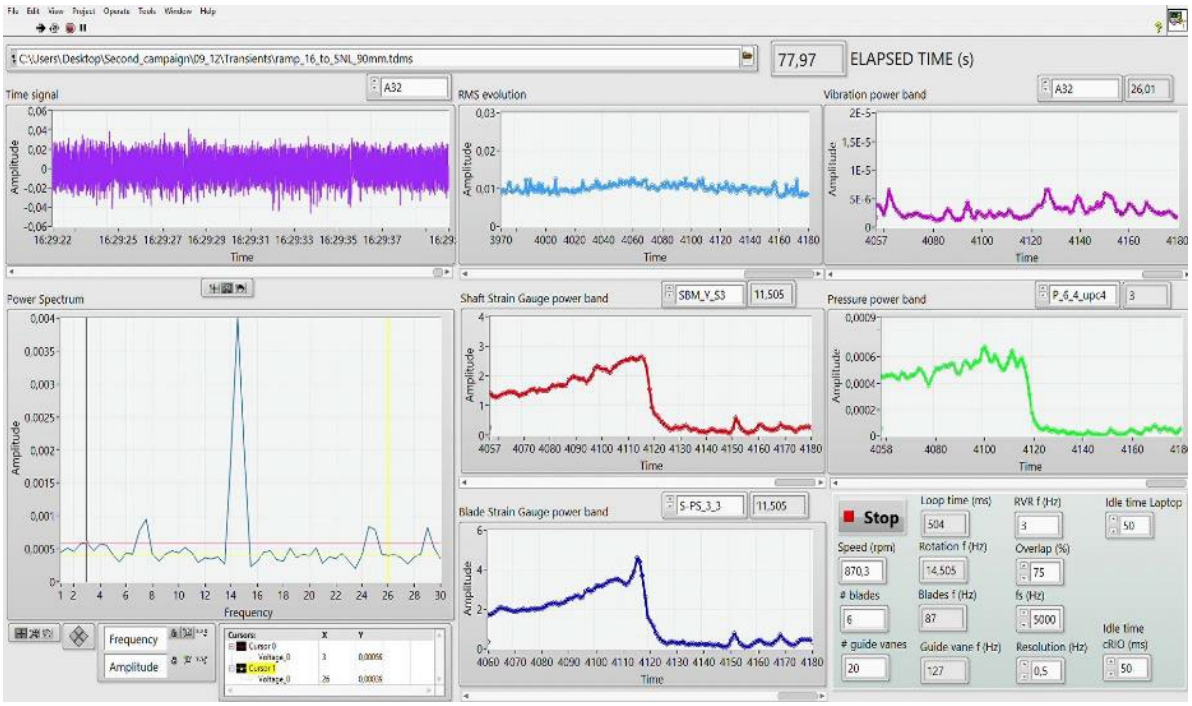

Figure 3 - Front panel of the SHM system to monitor in real time the indicators from the model turbine.

2.2 Results

Using the SHM system, the operating conditions with higher amplitude of the RVR could be identified, which mainly correspond to the 15º guide vane opening condition. Additionally, the start-up sequence was also be monitored using the SHM system, where the RVR frequency was also excited as it can be seen in Figure *4*.

Additionally, with the transient measurements, the damage induced at the blades of the turbine were also quantified applying the Rainflow counting algorithm. By doing so, it could be seen how the damage induced at the blade in the PS3 strain gauge, placed at the pressure side near to the hub, presented a higher level compared with the rest (see Figure *5*a). Additionally, the damage obtained with respect to BEP was also found to be higher at 15º than for the rest of Part Load (PL) conditions, being the highest for the SNL condition with cavitation (see Figure *5*b).

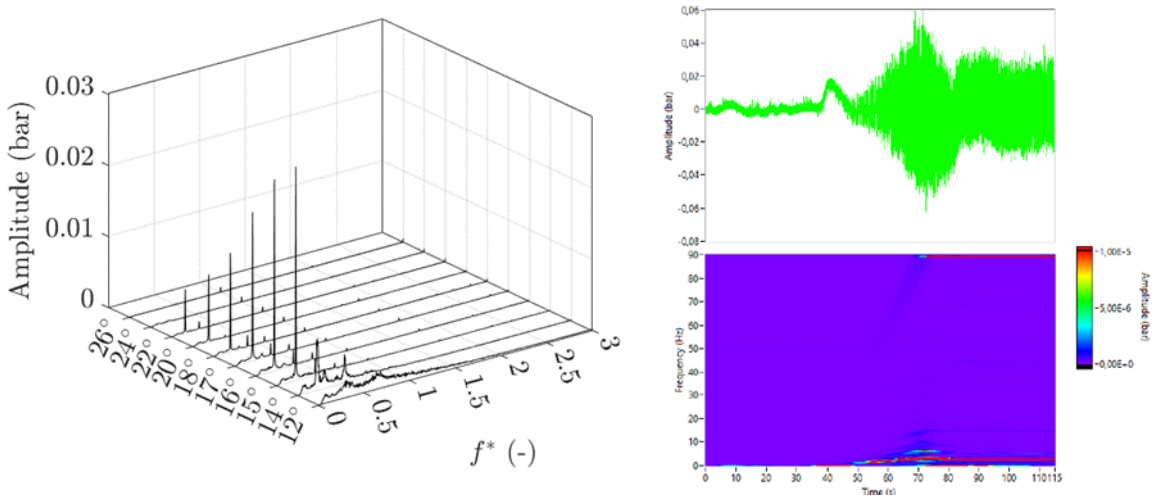

(a) (b)

Figure 4 - Spectra of the draft tube pressure pulsations at several GVO (a) and time signals and short time Fourier transform of the draft tube pressure (b). Image from [1] and [2].

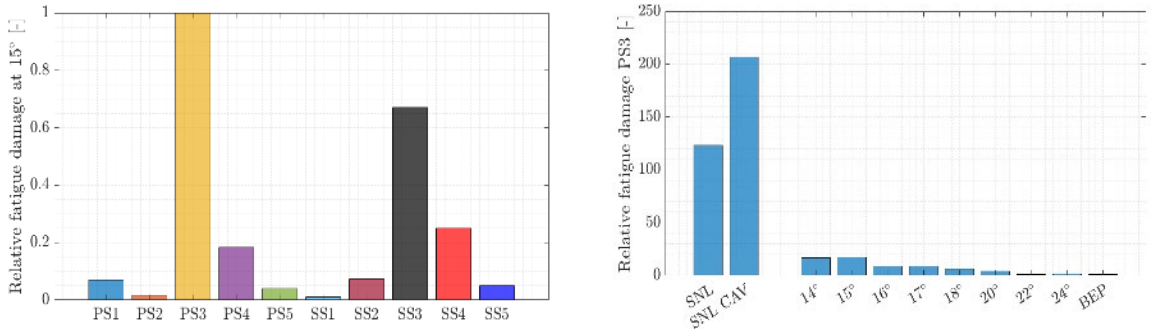

(**a**) (**b**)

Figure 5 - Fatigue damage at 15º of all the strain gauges mounted on the blade normalized with respect to PS3 (a) and at all operation conditions normalized with respect to BEP (b). Images from [3].

References

[1] Roig, R.; Sánchez-Botello, X.; Escaler, X.; Mulu, B.; Högström, C.-M. On the Rotating Vortex Rope and Its Induced Structural Response in a Kaplan Turbine Model. Energies 2022, 15, 6311. https://doi.org/10.3390/en15176311

[2] Escaler, X. *et al* 2022 *IOP Conf. Ser.: Earth Environ. Sci.* 1079 012059

[3] Roig R, Sánchez-Botello X, de la Torre O, et al. Fatigue damage analysis of a Kaplan turbine model operating at off-design and transient conditions. Structural Health Monitoring. 2023;0(0). doi:10.1177/14759217231191417

3 IPM subsystem

As one of the two flow control components incorporated into the AFC system, the IPM operates upon variable-length insertion of cylindrical rods into the draft tube. The initial design was based on the use of nozzles to inject pulsating jet flow into the draft tube flow field, as implied by the abbreviation IPM which stands for injection of pulsating momentum. The design was later modified to the radial protrusion of solid bodies, i.e., cylindrical rods installed on the draft tube to achieve flow field perturbation. The results of computational fluid dynamics (CFD) simulations performed at *Luleå Tekniska Universitet* (LTU) indicated that the protrusion of rods disrupts the rotating vortex rope (RVR) structure that forms in the draft tube under part-load operations. Being the main source of part-load pressure pulsations, the RVR perturbation thus leads to the mitigation of these oscillations as pursued in the project AFC4hydro.

The modified IPM concept was then experimentally investigated on a scaled-down model turbine at LTU. Four rods were protruded into the draft tube of a propeller turbine with a runner diameter of D= 100 mm at different lengths. The details of these experiments are presented in deliverable D1.2. Figure 6 shows one of the results obtained during the aforementioned tests.

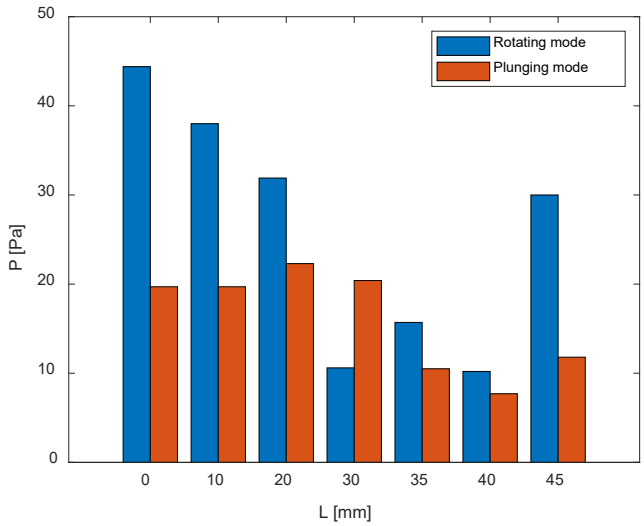

Figure 6 - The effect of rod protrusion on the RVR-induced pressure pulsation in the draft tube of the scaled-down model turbine.

Similar to the numerical simulations, downscaled model tests at LTU validated the potential of the IPM subsystem in mitigating the RVR and its consequent pressure oscillations. Moreover, these results demonstrated an optimum protrusion length where the highest RVR mitigation occurs. This allows optimization of the IPM action using a feedback-loop controller with the objective of obtaining the highest RVR mitigation. Consequently, the IPM was tested on a larger scale using a model turbine to see if similar effects can be observed and investigate the implementation of a controller. With a runner diameter of D= 400 mm, the studied model was a 1:3.875 scale of the U9 Kaplan turbine located at the Vattenfall R&D facility in Älvkarleby, Sweden.

3.1 System implemented

The designed IPM subsystem for the model tests consisted of four rods with a diameter of 0.15·D to be radially inserted into the draft tube. Four servomotors coupled with linear actuators were used to move the rods up to 170 mm inside the draft tube. Figure 7 displays the IPM rods in the model turbine draft tube along with the nozzles for the ICM subsystem.

The IPM subsystem was tested under WP1 at four different part-load conditions with different guide vane opening angles (α). The details of these tests and their results are reported in the deliverable D1.3. Under each condition, draft tube pressure measurements were performed at two axial locations (sections A and B) to quantify the amplitude of the pressure oscillations. Four piezoelectric pressure transducers (113B28 PCB) with a range of 344.7 kPa were installed at each section separated by 90 degrees around the draft tube periphery, see Figure 8.

Figure 7 - IPM rods and ICM nozzles inside the draft tube of the reduced scale model turbine.

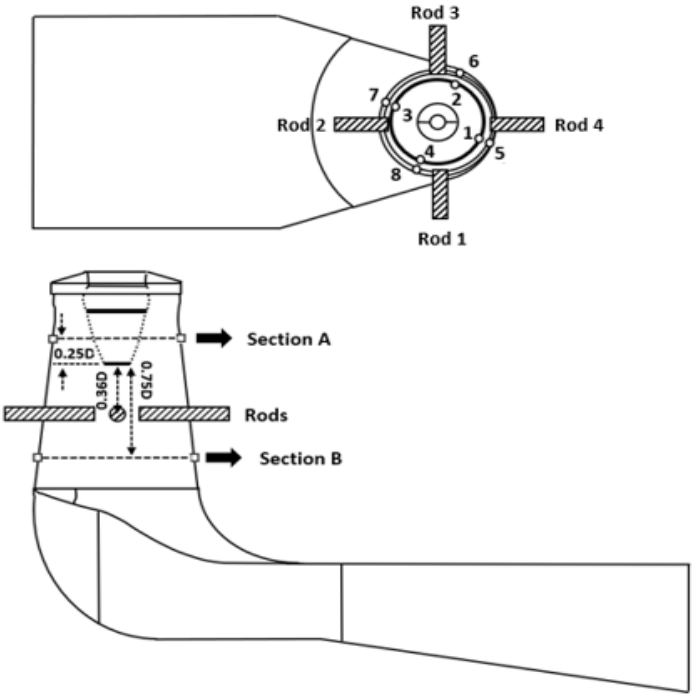

Figure 8 - Schematic view of the location of the pressure sensors and rods in the draft tube of the reduced scale model turbine.

During the IPM experiments under WP1, the rods were moved simultaneously from L= 0 mm to L= 170 mm at steps of 10 mm under each operating point while performing pressure measurements.

3.2 Results

The implementation of the IPM system on the model turbine led from partial to almost complete mitigation of the RVR-induced pressure oscillations under the different operating points. Nevertheless, under all conditions, an optimum protrusion length with the highest mitigation rate was observed. Figure 9 displays some results where the IPM implementation realized partial and/or significant mitigations in the form of Fourier spectra. The pressure amplitudes are normalized with the turbine net head while the frequencies are made dimensionless by the runner rotational frequency.

The maximum mitigation obtained under α= 20° was 85% while being only 15% under α= 16°. However, the WP1 experiments were performed under discrete protrusion lengths. Consequently, the implementation of the AFC system enables an active adjustment of the protrusion length to obtain the maximum attainable mitigation more precisely.

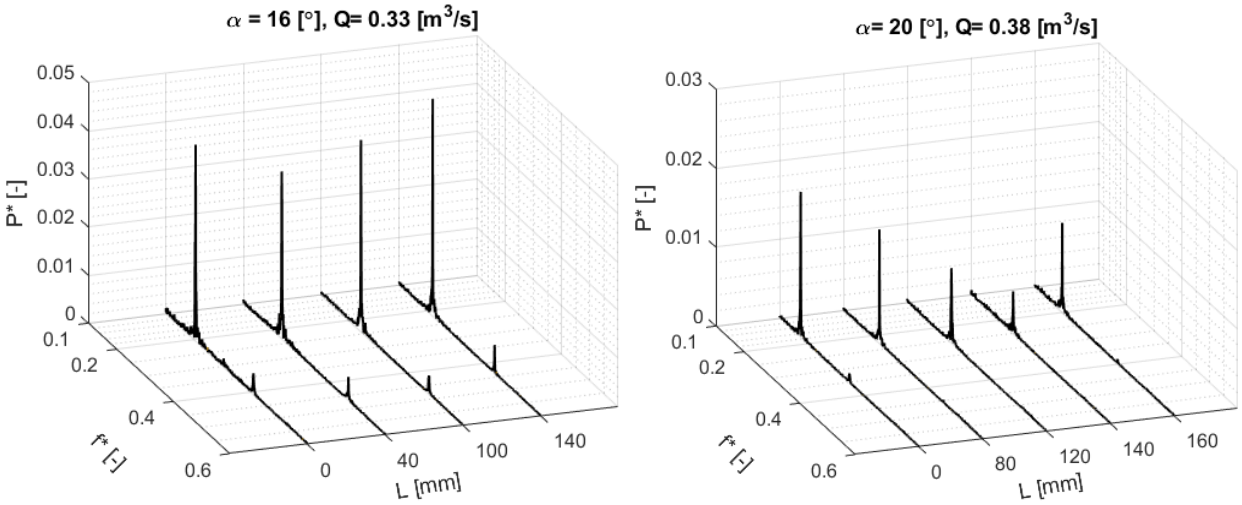

Figure 9 - Fourier spectra of the pressure oscillations from sensor 1 under the different operating conditions and protrusion lengths in the turbine model.

4 ICM

ICM together with IPM make up the pressure pulsation mitigation methods validated through AFC4Hydro. The ICM works on the basis that the amplitudes of the pressure pulsations, due to the Rheinganz or Rotating Vortex Rope (RVR) instabilities, depend on the Swirl number (S). Where S is the ratio between the flux of the integral average tangential momentum, $rc_T\rho c_Z dA$ and the integral average of the flux of axial momentum, $Rc_Z\rho c_Z dA$. The integral area (A) is a typical cross-section of the draft tube. c_T is the tangential speed in the plane (Z=constant). c_Z is the axial speed in the plane (Z=constant). r is the independent variable in the radial direction with r=0 in shaft-centerline. R is the radial extension on the plane (Z=constant).

The ICM established through AFC4Hydro now tries to manipulate S by modifying either the tangential or axial momentum and by angling the nozzle in the respective directions. Furthermore, we expect the associated amplitude to be a function of S and that a maximum pressure pulsation amplitude for a given S exists. In this setting the basic work of ICM is to kick the system away from the maximum amplitude.

Based upon work on the ICM 1st generation and ahead of the AFC4Hydro, FDB established a scaling formula for the required ICM injection flow rate (q):

$$q = C_{ICM} \cdot Q \cdot R \cdot \omega \cdot h^{-0.5}$$

Where C_{ICM} is a constant depending on the turbine unit type, speed number, unit maker etc. and the angular direction of the injected ICM jet flows. Q is the unit flow rate, R the turbine unit exit radius and ω the unit speed in rad/s. h is the pressure level, in mWc, of the injected water through the ICM nozzles.

Ahead of the testing at Älvkarleby, FDB used a different scaling formula adapted to high head Francis turbines. This variant turned out to predict too low flow rates for the required injection flows (q) in Kaplan units, and with the consequence of both running CFD prediction and many of the tests at Älvkarleby at flow rates (q) having little or any effects on the RVR.

4.1 System implemented

An important aspect of ICM during the AFC4Hydro included added degrees of freedom (DOF) for the operation of the angular adjustment of the ICM injection. The DOFs realized at Älvkarleby used many features that were to become the final design, see Figure *10*. An individual nozzle control was selected. A stepper motor was used for controlling the rotation of the nozzle, while a linear actuator was used to move the nozzle assembly. For the gears transferring motion between the stepper-motors and the ICM nozzle shaft, FDB selected to use 3D printed components. The 3D printing turned out to be less accurate than expected, and the gear slipped at times. This fact required manual intervention by resetting the system, and drive the nozzles a second time to the set-point position. We had to do frequent manual intervention something that made it difficult to perform the automatic solution for finding settings for optimum mitigation for a given turbine unit operation point.

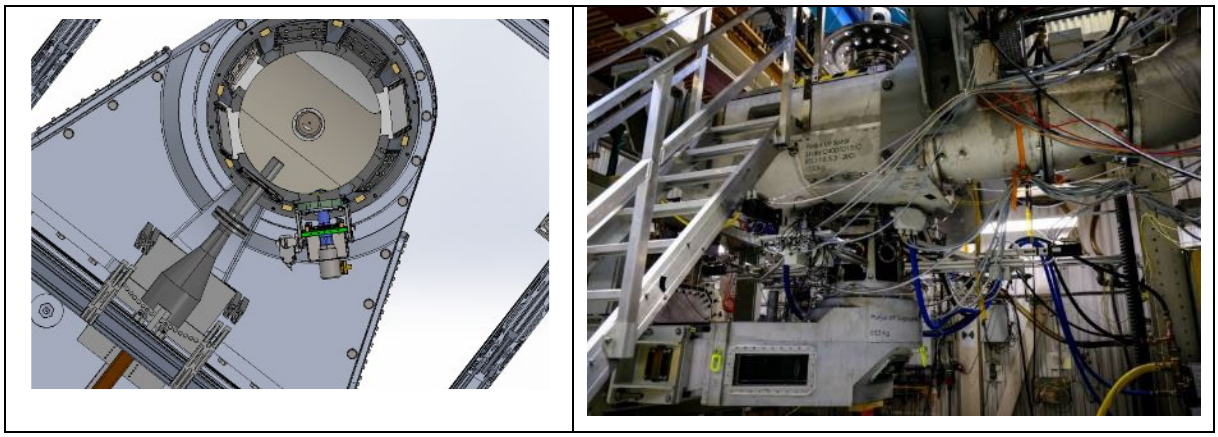

Figure 10 - (Left) 3D rendering of the IPM and ICM system installed in the draft tube cone at the Älvkarleby test facility. The graphics shown 1 of 4 for each of the two systems. (Right) The draft tube cone during testing; the systems themselves and bundles of cabling fill the space around the draft tube cone.

Given the relatively low head difference over the turbine model unit in Älvkarleby FDB decided to establish a pump system, controlled by a variable speed-drive, providing the required injection flow (q) and injection pressure (h) for the nozzles. Figure *11* shows the schematic of the pump skid, and an overview of all actuators and stepper motors (M) controlled and sensors used (P= pressure, S= position, F=flow).

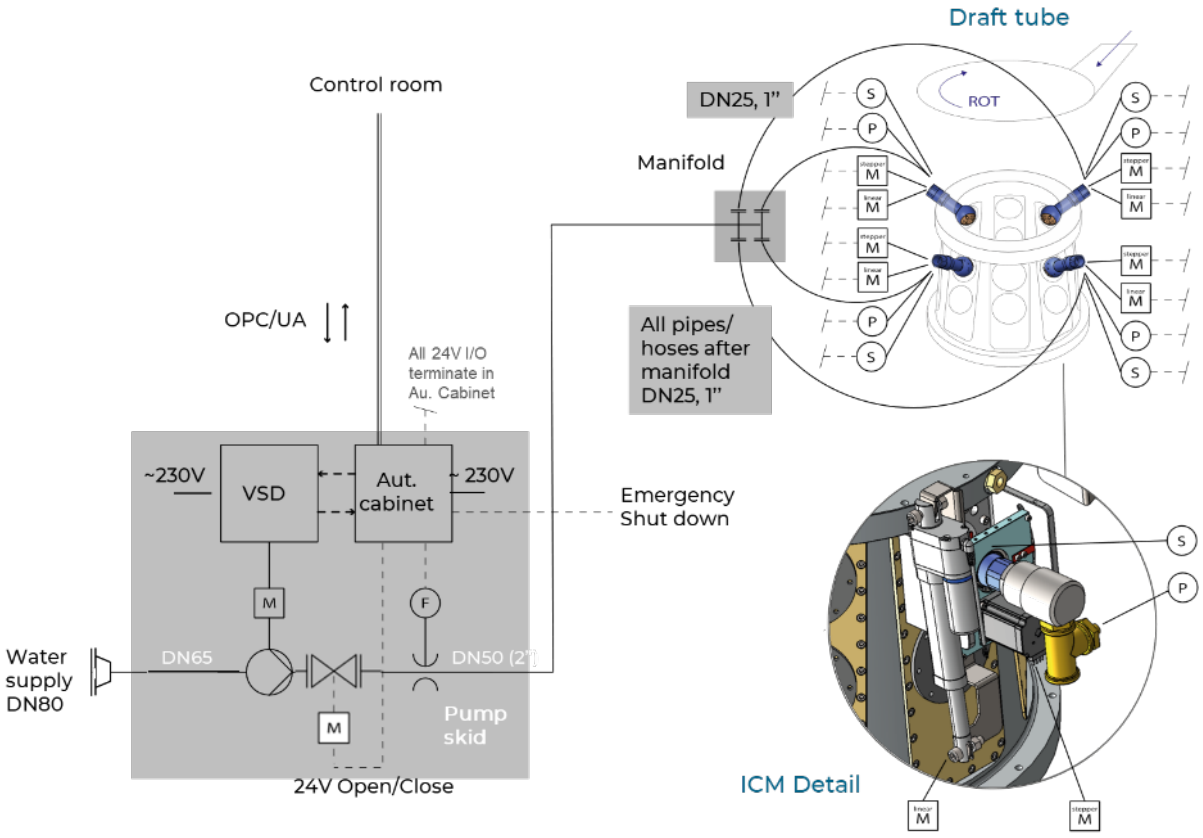

Figure 11 - ICM system set up at Vattenfall turbine model test facility in Älvkarleby.

4.2 Results

An experimental matrix with a mix of injection flow rates (q), nozzle openings, injection pressures (h) and angular positioning of the nozzle injection (s_{Tan}, s_{Ax}) was completed during ICM tests at Älvkarleby. Figure *12* shows selected results from the test that served as a link when scaling results between turbine model and prototype (Porjus). At this point during the campaign in Älvkarleby the configuration used for ICM and the operation of the turbine unit mimicked those expected in Porjus. Figure *12* shows the impact of ICM on the pressure dynamics measured at two horizontal (z=const) planes, where green markings indicate readings in the plane closer to the runner and the blue markings indicate readings in a plane below the ICM nozzles.

The results showed that ICM had a positive impact on mitigation of pressure pulsations at GVO =11°, and for a scaled injection flow rate and pressure (q, h) that was calculated for the pumps hired for the Porjus campaign.

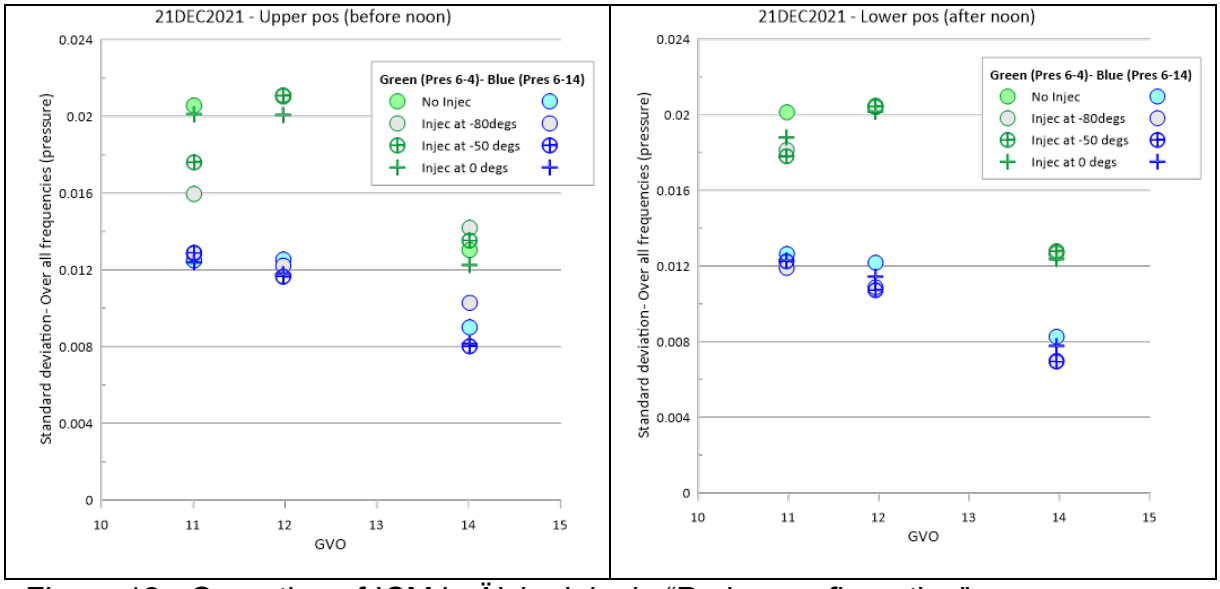

Figure 12 - Operation of ICM in Älvkarleby in “Porjus configuration”.

5 Controller

Optimizing vortex mitigation is crucial for maintaining the efficiency and longevity of hydroturbine systems. To address this challenge, we introduce an intelligent control and optimization strategy that enables the hydro turbine to make informed decisions regarding vortex mitigation. This control strategy involves a two-layer operation consisting of the Operational Layer and the Optimization Components, which work together to ensure optimal performance and vortex mitigation in the hydroturbine system (Figure 13).

Furthermore, this proposed approach exhibits versatility by being applicable in both the Injection of Pulsating Momentum (IPM) and Injection of Continuous Momentum (ICM) scenarios. Leveraging Structural Health Monitoring (SHM), the system acquires crucial data about the turbine's status, enabling it to make informed decisions regarding vortex mitigation. Additionally, the optimized layer can seamlessly receive optimization objectives from the SHM unit, facilitating the minimization of critical parameters as needed. This adaptability and integration of sensor technology underscore the cutting-edge nature of our control and optimization strategy for hydro turbines.

The control and optimization strategy for vortex mitigation in hydro turbines is a sophisticated two-layer system designed to manage the turbine's operation efficiently and respond to changing conditions. These layers are as follows:

a. Operational Layer:

The Operational Layer serves as the primary decision-maker in the system's normal mode of operation. This layer continuously monitors the operational status of the hydro turbine plant, collecting data and evaluating the need for vortex mitigation. The critical function of this layer is to decide on the optimal control signal for the turbine based on real-time information.

This decision-making process relies on a stochastic process that predicts optimal control values based on the operational conditions and assesses the confidence associated with these predictions. If the Operational Layer determines that the confidence in the current optimal estimate is insufficient, it triggers the activation of the Optimization Components.

b. Optimization Components:

The Optimization Components represent the second layer of the system and come into play when the Operational Layer identifies a need for optimization. These components are responsible for refining the control signal and optimizing the vortex mitigation strategy.

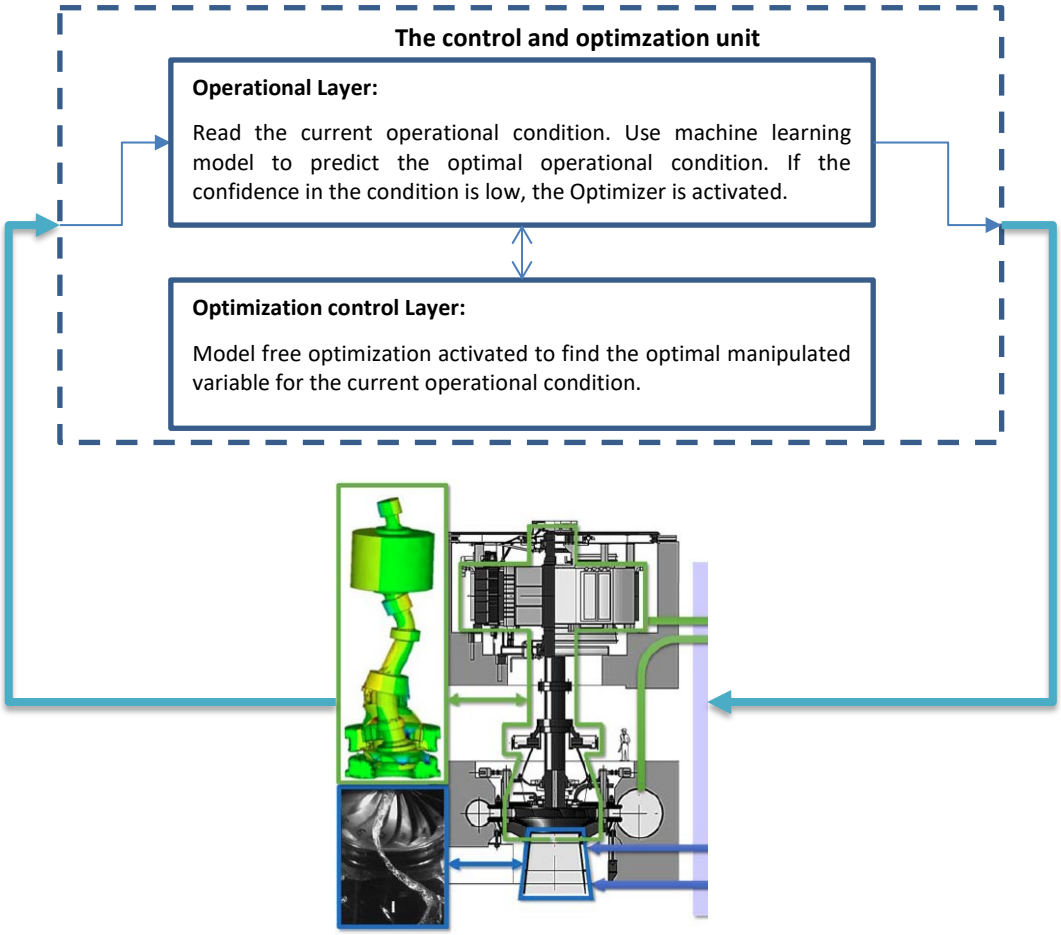

Figure 13 - The proposed controller structure that consists of the operational layer and the optimization layer.

The control and optimization strategy for vortex mitigation in hydro turbines follows a systematic approach comprising three distinct stages to ensure optimal performance and vortex mitigation. These stages are as follows:

Regular Operation and Optimal Prediction:

In the first stage, the system operates in normal mode, continuously monitoring the operational status of the hydro turbine plant. During this phase, the Operational Layer leverages a stochastic process to predict the optimal control signal. The system estimates the optimal values and assesses the associated confidence level by sampling and analyzing the stochastic process. It remains in this mode as long as the confidence in the optimal estimate remains within acceptable bounds.

Transition to Optimization Mode:

When the Operational Layer detects a discrepancy or uncertainty in the current control signal's effectiveness in mitigating vortex-related issues, it initiates the second stage: the transition to optimization mode. This transition is crucial for fine-tuning the control strategy to ensure optimal performance. The Optimization Components come into play during this stage, working diligently to optimize the vortex mitigation strategy.

Stochastic Process Update and Learning:

The third stage involves updating and learning from the optimization process. Once the Optimization Components have completed their task, the system updates the operational layer's stochastic process. This update incorporates the knowledge gained from the optimization, enhancing the system's ability to make more accurate decisions in future operational cycles. The learning process ensures continuous improvement and adaptability, making the control and optimization strategy a dynamic and intelligent hydro turbine vortex mitigation solution.

In summary, the control and optimization strategy for vortex mitigation in hydro turbines is a sophisticated and intelligent system that operates in two layers: the Operational Layer and the Optimization Components. This strategy ensures that the hydro turbine can effectively manage vortex-related issues, optimizing its performance and minimizing operational disruptions. By continuously assessing the need for optimization and updating its decision-making process, this control system stands at the forefront of hydroelectric power generation technology, ensuring hydro turbines' efficient and reliable operation.

5.1 System implemented

Implementing our vortex mitigation control and optimization strategy leverages high-level tools and technologies. These tools play a vital role in ensuring the effectiveness and adaptability of the system. Below, we detail the key components used in the system:

1. Stochastic Processes - Gaussian Process:

Gaussian processes serve as the cornerstone of the system's stochastic processes, offering several key advantages over other machine learning tools:

- Probabilistic Modeling: Gaussian processes provide a probabilistic framework for modeling and predicting optimal control values along with their associated uncertainties. This inherent probabilistic approach allows the system to capture and work with the inherent variability found in real-world systems.
- Flexibility and Adaptability: Gaussian processes are highly adaptable and versatile, making them suitable for scenarios where system behavior may change over time. This adaptability ensures the system can adjust to evolving conditions in hydro turbine operation.
- Efficient Exploration: Gaussian processes enable efficient exploration of the parameter space. They guide the system to sample points where optimal control values are likely to be found, reducing the number of experiments or iterations required to achieve desired performance.
- Uncertainty Quantification: Gaussian processes naturally quantify uncertainty in predictions. This feature is critical for informed decision-making, allowing the system to assess the confidence in estimated optimal operating parameters. This confidence assessment plays a vital role in determining when to transition to optimization mode, ensuring well-informed decisions.

Gaussian processes offer a robust and efficient approach to optimizing vortex mitigation in hydro turbines, thanks to their probabilistic modeling capabilities, adaptability, and ability to handle uncertainty effectively.

2. Optimizer Approaches:

   The optimization component of our system employs two distinct approaches to fine-tune the control strategy:

   - Phasor Extremum Seeking Control: Phasor Extremum Seeking Control is a model free dynamic optimization technique that continuously adjusts control parameters to seek the Extremum of a performance metric. It allows the system to actively optimize vortex mitigation in real time by dynamically adapting control signals to achieve optimal performance. It offers advantages over classic control methods, including real-time adaptation, performance optimization, reduced manual tuning, and enhanced system robustness. This makes it an ideal choice for optimizing vortex mitigation in hydro turbines.
   - Gaussian Processes and Bayesian Optimization: Bayesian optimization provides a data-driven approach in conjunction with Gaussian processes. It uses probabilistic models to guide the search for optimal control settings efficiently. This approach enables the system to explore the parameter space effectively and adapt to changing conditions for improved vortex mitigation. The combination of Gaussian processes and Bayesian optimization offers several key advantages:
     - Probabilistic Modeling: Gaussian processes provide probabilistic modeling, enabling the system to capture uncertainties and quantify confidence in control settings.
     - Efficient Exploration: Bayesian optimization efficiently explores the parameter space, reducing the number of experiments needed to find optimal settings.
     - Adaptability: The system can adapt to changing conditions by continuously updating its model with new data.
     - Dynamic Decision-Making: Bayesian optimization balances exploration and exploitation dynamically for optimal vortex mitigation.
     - Enhanced Optimization Objectives: The system can focus on specific optimization goals, making it versatile for various hydro turbine scenarios.

5.1.1 Implementation Platform:

The core of our system was implemented using LabVIEW, a powerful graphical programming environment ideal for control and automation applications. This platform provides a user-friendly interface for system design and integration.

The controller, responsible for real-time decision-making, runs on the Compact RIO (Real-Time Input/Output) hardware platform. This ensures that control actions are executed promptly to respond to the dynamic nature of hydro turbine operation.

The main Bayesian optimization and stochastic processes are implemented using MATLAB code, which operates within LabVIEW on the host PC. These MATLAB components communicate seamlessly with the Compact RIO over Ethernet,

facilitating data exchange and decision synchronization between the host PC and the control hardware.

This comprehensive implementation approach combines advanced mathematical modeling with real-time control capabilities, enabling our system to make informed decisions, optimize vortex mitigation, and adapt to varying conditions in hydro turbine operation. The synergy of these tools ensures the efficiency and reliability of our control and optimization strategy.

5.1.2 The phasor Extremum seeing control implementation:

The Phasor Extremum Seeking Control (Phasor ESC) subsystem has been implemented within LabVIEW. This implementation features a user-friendly front panel and interface, making it adaptable for standalone use or seamless integration with other system components. To understand the implementation better and visualize the system in action, refer to the accompanying figures showcasing the one-dimensional case. These figures provide insights into the user interface and the system's functionality.

For comprehensive technical details and further information, please consult the deliverable D4.2. It contains a more in-depth description of the Phasor ESC implementation (Figure 14 and Figure 15), ensuring a thorough grasp of this critical component within our vortex mitigation control and optimization strategy.

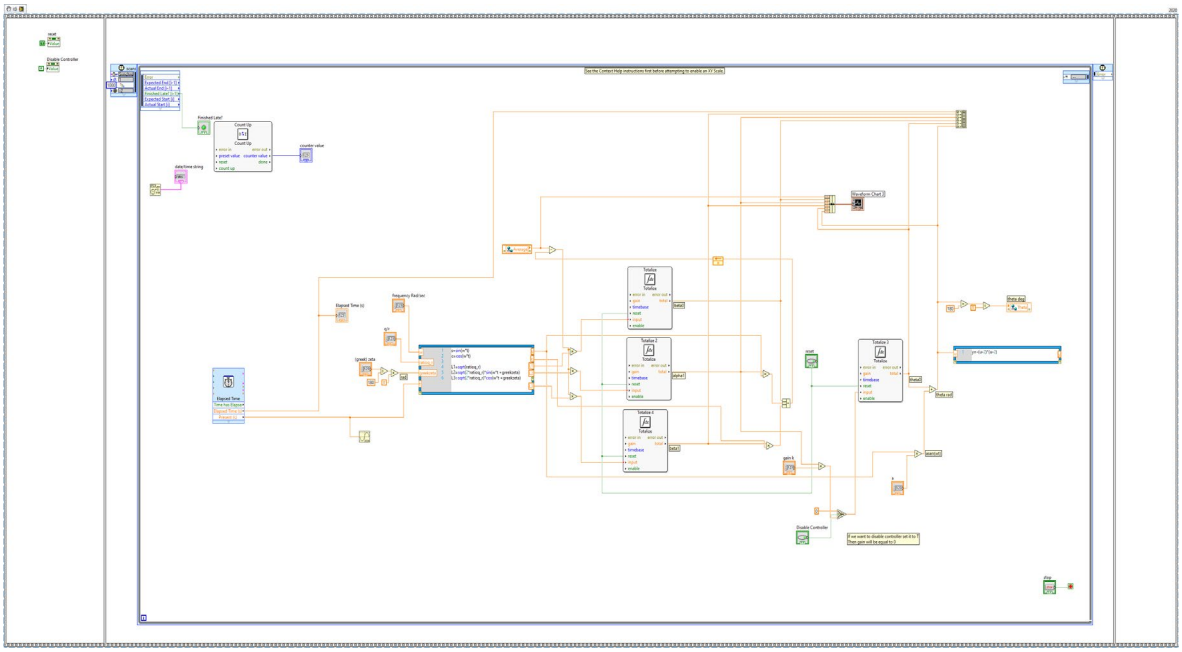

Figure 14 - The one-dimensional Phasor ESC that is implemented in LabView

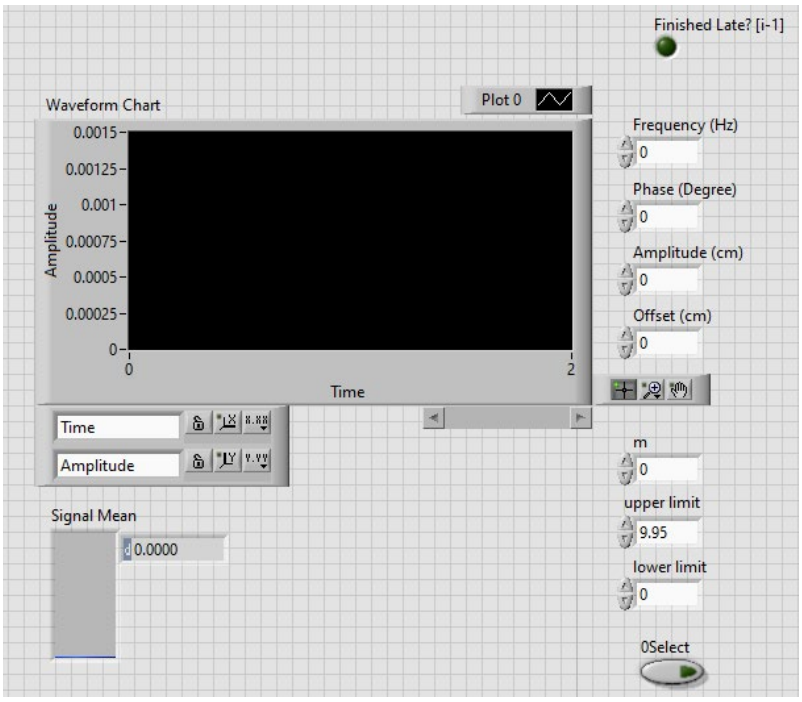

Figure 15 - The web interface of the phasor ESC component

5.1.3 Implementation of GP Optimization:

The optimization process in our system is divided into three distinct phases, each serving a crucial role in achieving optimal vortex mitigation:

1. Create Prior (Figure 16): During the "Create Prior" phase, the system establishes an initial probabilistic prior for the optimization problem. There are various approaches to determine this prior, with a commonly used option being a flat prior. A straightforward method involves sparsely sampling the parameter space, either randomly or linearly, and evaluating the cost function at these sampled points. This initial exploration sets the foundation for subsequent optimization steps.

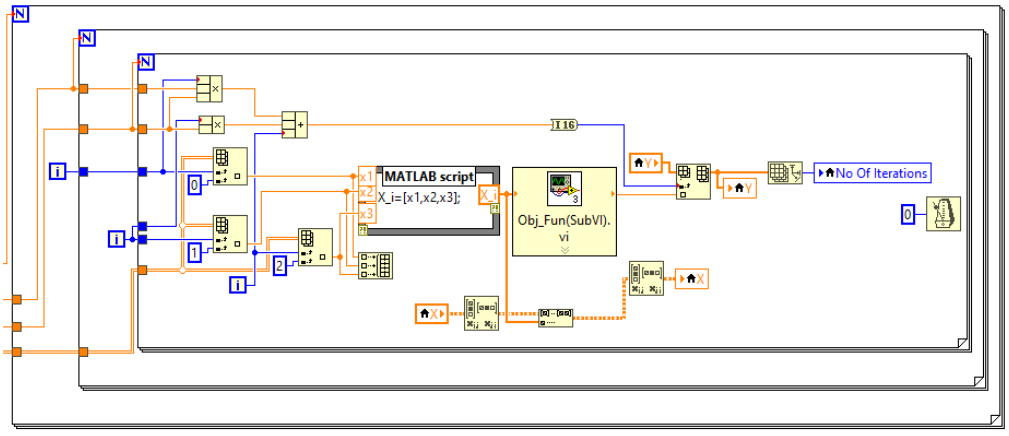

Figure 16 - The initial create Prior code part

2. Explore (Figure 17): In the "Explore" phase, the primary objective is to enhance confidence in the regression model before progressing to the optimization step. A regression model is initially constructed using the data collected during the "Create Prior" phase. The point with the minimum fitting confidence in the model is selected for further sampling. Subsequently, the regression model is updated with the new sampled information. This process is iteratively repeated, with the minimum confidence point being selected again for sampling. The termination criteria for this phase can be defined either when the confidence level in the operational space reaches a predefined threshold or when a maximum limit on the number of samples is reached.

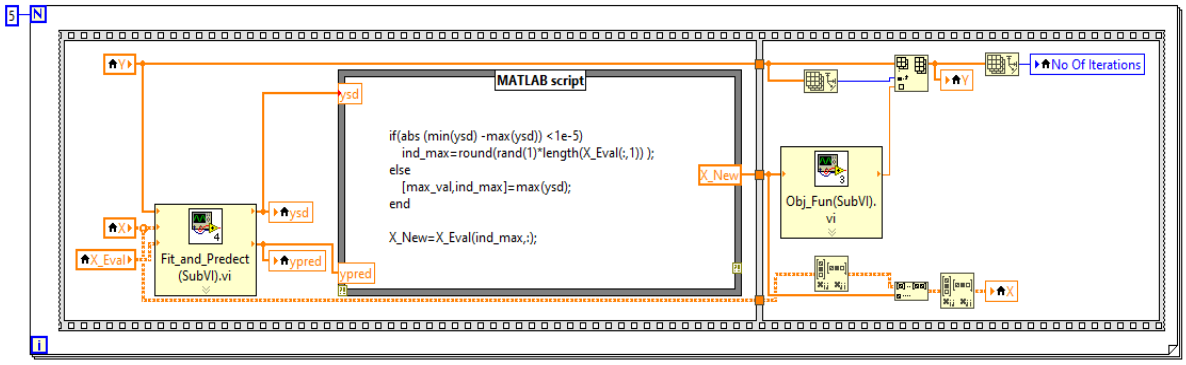

Figure 17 - Explore code implemented in LabView with integrated Matlab code

3. Exploit (Figure 18): The "Exploit" phase's primary objective is to identify the operational point that maximizes vortex mitigation. This phase utilizes the previously established confident regression model to find the extremum operational point. A search algorithm is applied to the Bayesian process, which is typically cheaper and faster to sample compared to the original process. Once the optimal candidate is identified, the actual process is sampled, and the Gaussian process is updated. This optimization phase is repeated iteratively until convergence to the same optimal point is achieved.

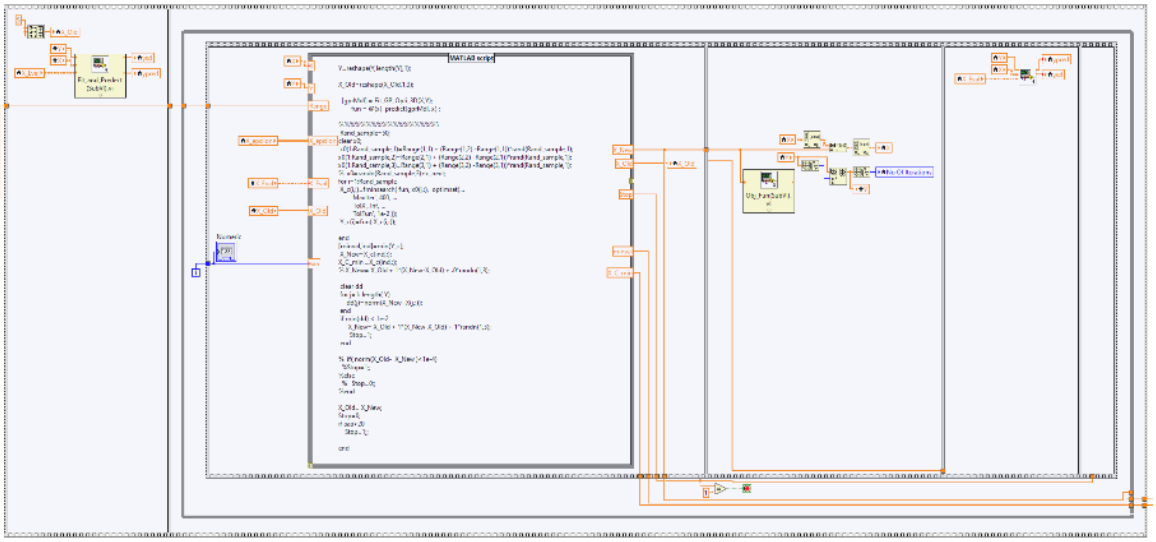

Figure 18 - Exploit code implemented in LabView with integrated Matlab code.

These three well-defined phases of create, explore, and exploit are integral to our Gaussian process-based optimization strategy, ensuring a systematic and efficient approach to optimizing vortex mitigation in hydro turbines. The process flow is carefully designed to maximize the system's ability to adapt and perform optimally in a dynamic operational environment (Figure 19).

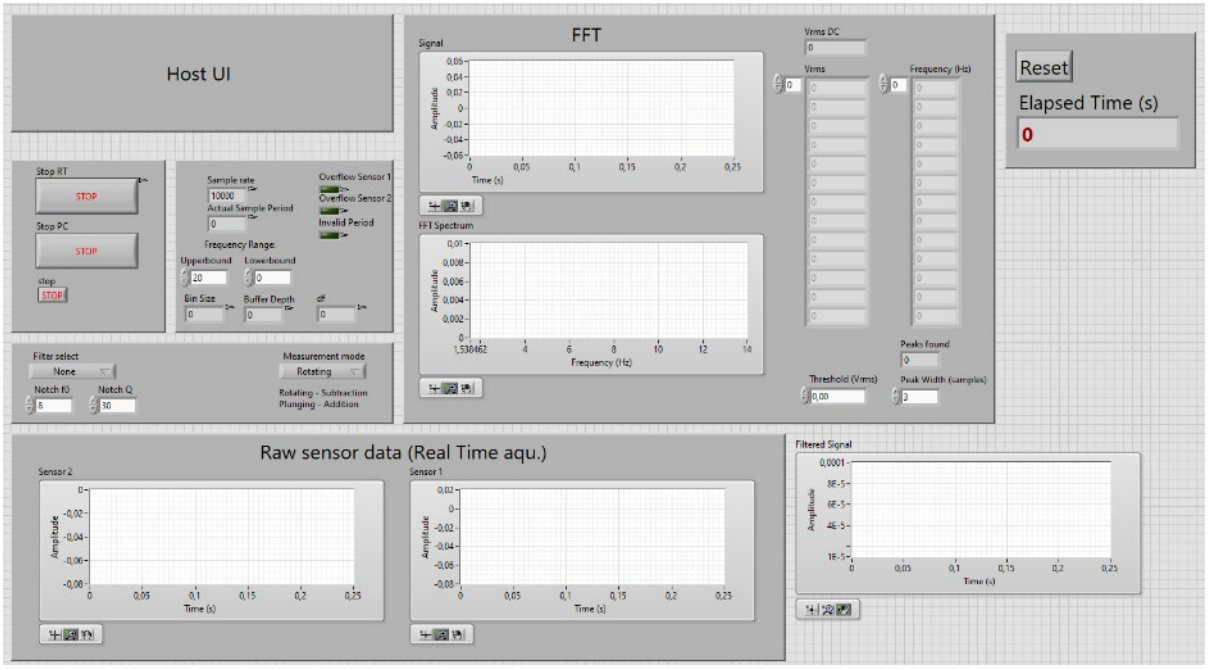

Figure 19 - User interface for rthe FFT tool that enable online tracking of the maximum frequncy component.

5.2 Results

In our experimental study, we focused on a Kaplan turbine model, aiming to measure its operational status, which can be quantified by key variables, including:

- Net Head: This parameter help determine the turbine's efficiency and performance.
- Guide Vane Angle: The angle of the guide vanes influences the flow of water into the turbine, affecting its operation.
- Turbine Blade Positions: The positions of the turbine blades directly impact power generation and vortex formation.

Our primary objective was to develop a stochastic process that could effectively map the turbine's operational status to an optimal rod insertion strategy. This mapping is crucial for enhancing vortex mitigation and optimizing turbine performance.

In line with our experimentation, we employed the Injection of Pulsating Momentum (IPM) approach to investigate rod insertion configurations. Our test cases encompassed two scenarios:

1. Uniform Rod Insertion: In the first set of tests, we assumed that all rods were inserted with the same length. This configuration allowed us to evaluate the performance and efficiency of the turbine when all rods contribute equally to vortex mitigation.
2. Three Degrees of Freedom: In the second set of tests, we introduced three degrees of freedom for rod insertion. Specifically, we varied the insertion lengths of two rods equally, while the remaining two rods had individual insertion lengths. This configuration provided insight into the impact of asymmetric rod insertion on vortex mitigation and turbine efficiency.

Our experimentation aimed to validate the effectiveness of the stochastic process and the IPM approach in optimizing rod insertions for vortex mitigation. The results of these tests will shed light on the most efficient strategies for enhancing the performance and reliability of Kaplan turbines in real-world operational conditions.

Objective selection:

The core objective of our testing revolved around optimizing vortex mitigation, focusing on one of two key metrics: either the maximum frequency component within a defined frequency band or the energy contained within a specific frequency range in the region of interest. These metrics served as critical indicators for the effectiveness of our optimization process.

In the first approach, we harnessed online Fast Fourier Transform (FFT) tools to track the vortex frequency in real time. This method allowed us to continuously monitor and adjust the turbine's operation based on the maximum frequency component within the target frequency band. To ensure precise and rapid execution of the FFT analysis, we implemented it using the Field-Programmable Gate Array (FPGA) of the Compact RIO (CRIO) platform. This FPGA-based approach ensured accuracy and efficiency in tracking vortex frequencies.

Conversely, the second approach relied on filter-based techniques to measure the energy within a designated frequency band. This method offered an alternative

means to assess the effectiveness of vortex mitigation strategies, particularly in scenarios where pressure signals within the draft tube were of interest. By quantifying the energy of signals within the specified frequency range, we could ascertain the performance of our optimization process in minimizing vortex-related phenomena.

These two distinct approaches provided valuable insights into the optimization of vortex mitigation, offering complementary methods for evaluating and improving the performance of Kaplan turbines under varying operational conditions. The diagram is shown in Figure *20*.

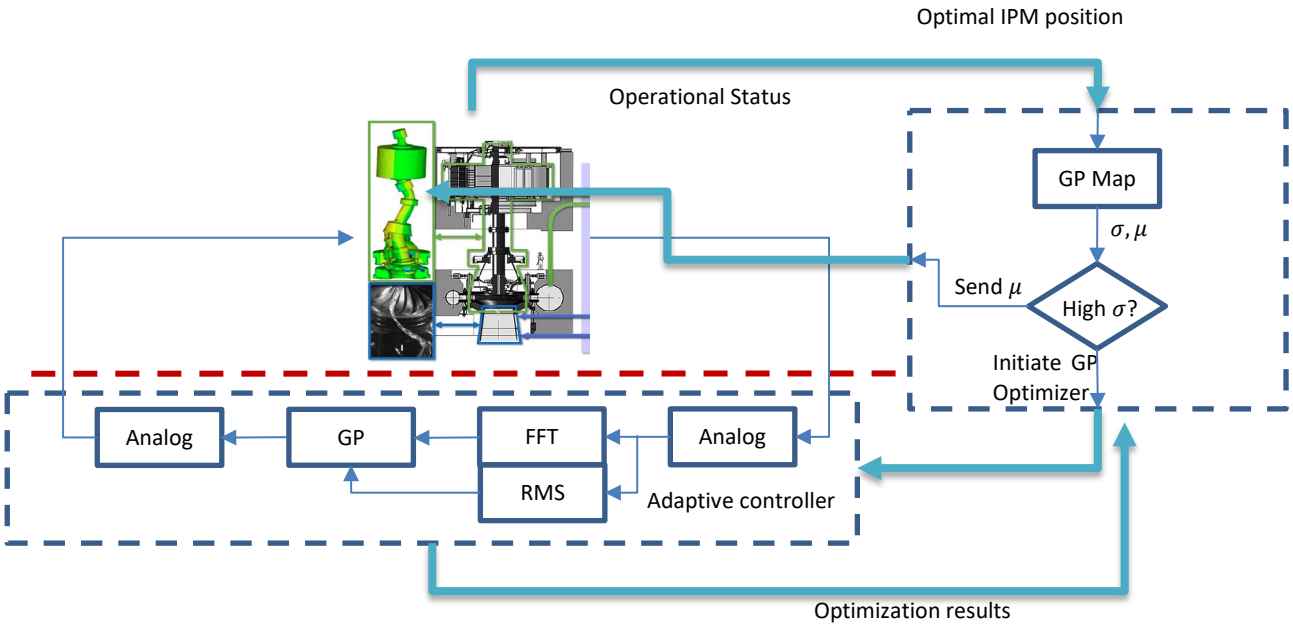

Figure 20 - The integration of the mapping with the optimizer and showing the 2 Optimization Objective Metrics for Vortex Mitigation

In the conducted tests, the Gaussian Process (GP) optimizer demonstrated its capability to identify optimal rod insertions for specific operational scenarios, as illustrated in Figure *21*. The GP optimizer efficiently explored the parameter space by leveraging the chosen objective metrics—minimizing the maximum frequency component within a defined. The results highlight its ability to adapt rod insertions in response to the dynamic operational conditions of the Kaplan turbine. These findings underscore the effectiveness of our optimization approach in achieving vortex mitigation across a range of practical scenarios, showcasing the GP optimizer's potential for enhancing turbine performance and reliability.

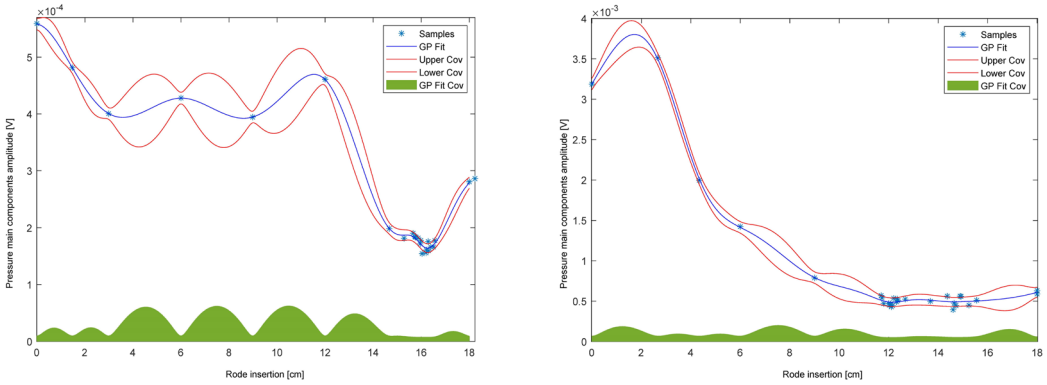

Figure 21 - Gaussian Optimizer Results for Two Different Guide Vane Positions: This figure illustrates the Gaussian optimizer's proficiency in executing the three key phases outlined earlier. The final phase showcases the exploitation around the optimal point. The lower section features a confidence plot, providing insights into the Gaussian process's estimation confidence across the entire operational range.

The update of the stochastic process in one dimension is exemplified in *Figure 22*, showing the optimal rod insertion strategy in conjunction with variable guide vanes for specific head and blade position conditions. This representation vividly illustrates the adaptability and precision of the stochastic process, as it dynamically refines rod insertions to optimize vortex mitigation within the defined operational parameters. The figure provides a tangible testament to the system's ability to make informed decisions in real-time, further enhancing the performance and efficiency of the Kaplan turbine.

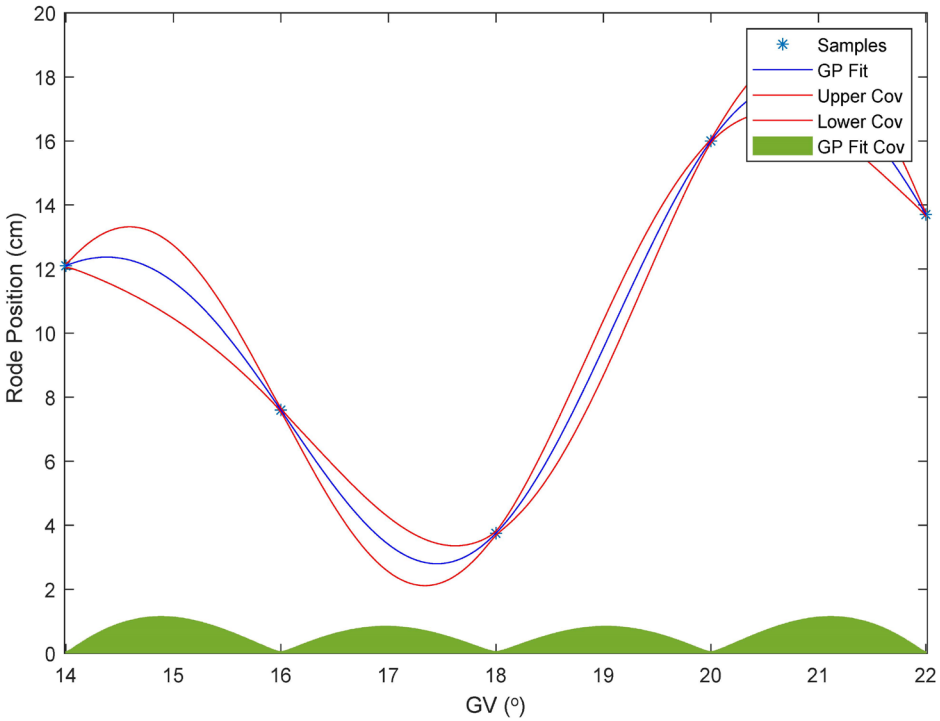

Figure 22 - Stochastic Process in One Dimension: Demonstrating Optimal Rod Insertion with Variable Guide Vanes for Specified Head and Blade Position. The figure depicts the outcomes of extensive sampling across the entire range of guide vane positions, utilizing five samples for optimal solutions. The green-shaded region represents the confidence interval for non-measured guide vane values. The Operational Layer plays a pivotal role in determining the trustworthiness of these values, triggering optimizer activation when necessary.

6 AFC system

The different subsystems; the Injection of Pulsating Momentum (IPM), Injection of Continuous Momentum (ICM), Structural Health Monitoring System (SHM), and the controller were developed at the Vattenfall water laboratory.

The SHM subsystem has the capability to calculate diverse real-time damage indicators tailored to the specific rotating speeds, blade and guide vane numbers, and dynamics of each prototype. These indicators can be monitored through spectra of a chosen signal, orbits of shaft displacement, or vibrations and power bands related to pressures, vibrations, strains, and/or shaft displacements. The IPM subsystem facilitates the reduction of pressure pulsations from the rotating vortex rope at all investigated operating points, with a potential complete mitigation. The ICM subsystem demonstrated some level of mitigation at lower operating condition. Finally, the controller continuously is able to continuously assess the need for optimization and updating its decision-making process for an optimal operation of the turbine based on measurements performed by the SHM to control the IPM and ICM.

Each subsystem development was performed with another subsystem, e.g., IPM with SHM, ICM with SHM and controller with IPM and SHM. Such results were presented in the previous sections.In the following, some preliminary results including the SHM, IPM and ICM are presented.

The complete AFC could not be tested because of time limitations. Nonetheless, the delopments performed at this stage are satisfactory.

6.1 Preliminary results without controller

The strain gauges mounted on the runner blades were used to assess the fatigue damage suffered relative to the operation at BEP. Among the triaxial strain gauge rosettes mounted on different locations at both pressure and suction sides of the instrumented blades, it was determined that the one placed on the pressure side in the closest location to the hub, named PS3, was the one suffering the most significant strain levels. Hence, the principal stress direction was computed from it after cleaning the noise of the signal using the Savitzky-Golay method.

Figure 23 shows the peak-to-peak evolution of the principal strain of PS3 during a ramp-up of load from SNL to BEP without any actuation (blue line) and with the actuation of the IPM and ICM systems. In this case, two maximum peak-to-peak amplitudes are reached around 13º and 15º, being the latter one the highest. With different rod protrusion lengths, the amplitude of both peaks is reduced and the guide vane opening at which the second peak occurs also changes. For instance, the rod protrusion of 90 mm (purple line) produces the maximum reduction of the second peak, moving as well the guide vane angle at which it occurs, whereas the protrusion of 150 mm minimizes more the first peak.

The damage induced in the blade during that transient between SNL and BEP can also be quantified applying the rainflow analysis to the signal filtered around the frequency of the RVR, obtaining the relative fatigue damage as presented in Figure 24. In this case, we can see how during the ramp-up (blue bars) the AFC systems work much better than during the ramp-down (orange bars), producing a higher reduction of the fatigue damage when the ramp starts from SNL. Additionally, it can

also be quantified from a fatigue point of view how the rod protrusion of 90 mm achieves a higher damage reduction than the rest of lengths, even producing more damage with the full rod protrusion of 150 mm during the ramp-down. It is also observed how the ICM also provokes a reduction of damage during both ramp-up and ramp-down transients.

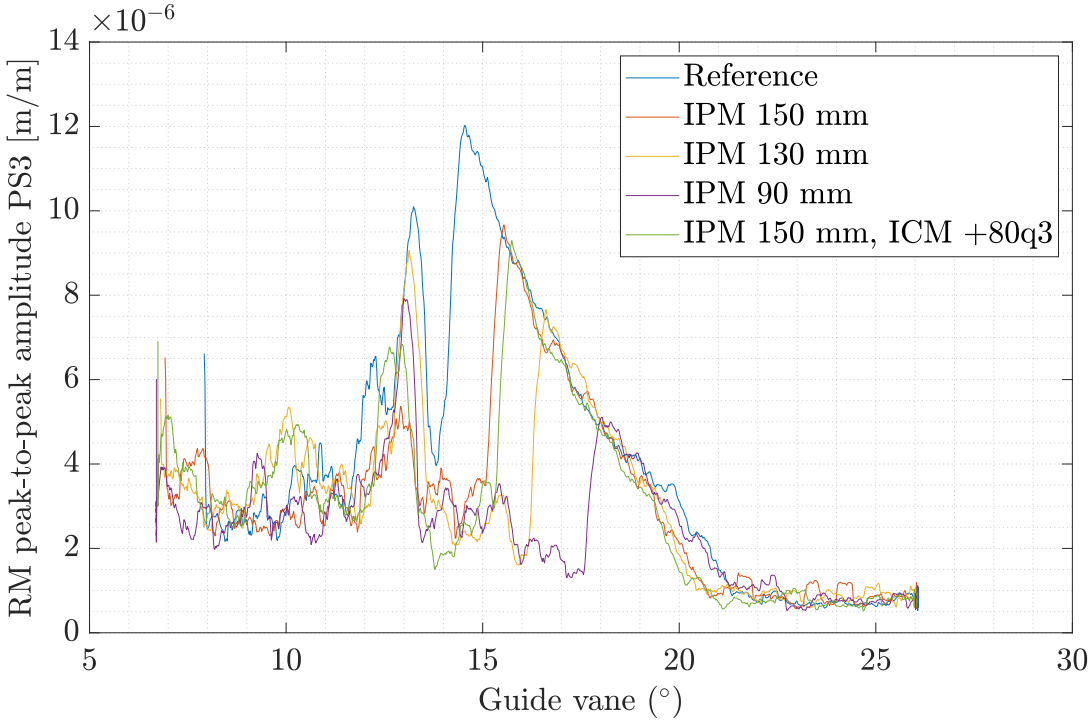

Figure 23 - Peak-to-peak amplitude of the blade strain gauge PS3 without and with the AFC systems during a ramp-up of load, filtered around the frequency of the rotating mode of the RVR.

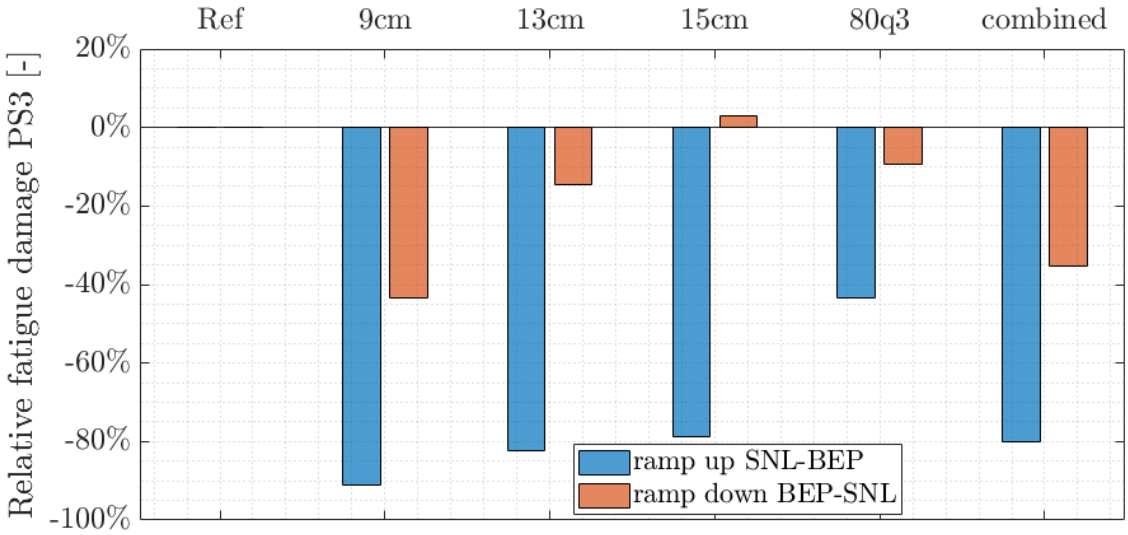

Figure 24 - Relative fatigue damage computed from the blade strain gauge PS3 with the AFC systems during ramp-up and ramp-down transients, filtered around the frequency of the rotating mode of the RVR.

Looking more in detail at the stationary part load operating condition corresponding to a guide vane opening of 14º, Figure 25 shows the reduction of fatigue damage calculated from the PS3 with the different injection systems. In this case, it can be seen how the rod protrusion of 150 mm achieves the highest reduction among the different tested protrusion lengths. On the other side, the fatigue reduction on the blade is also very sensitive to the angle of injection of the ICM system. It can be observed that the injection of 6 l/s in the runner rotation sense (“80q6”) produces more damage than the reference case without injection. On the other side, the ICM injection shooting partly axially and against rotation (“-50q6”) produces the highest fatigue damage reduction, meanwhile the injection fully against rotation (“-80q6”) presents less reduction. Finally, in this specific operating point it can be seen how the combined effect of IPM with 120 mm and ICM at condition -80q6 presents the highest fatigue damage reduction.

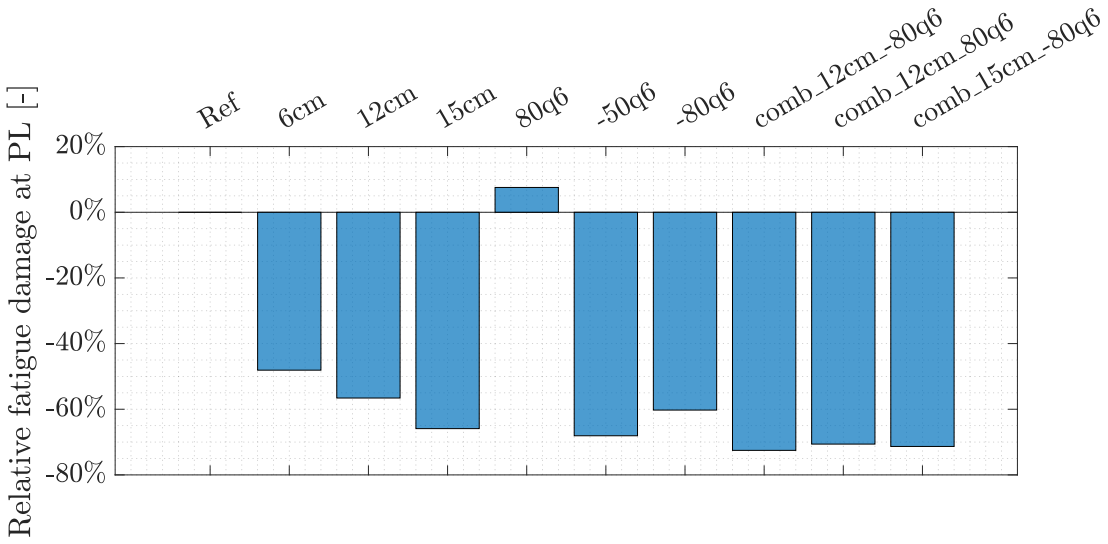

Figure 25 - Reduction of the fatigue damage computed from the blade strain gauge PS3 at 14º GVO using IPM and ICM systems separately and combined.